Multi-Factor Rainfall Thresholds (MF-RT) for shallow slip prediction based on field monitoring

Marianna Pirone[1,a], *Gianfranco* Urciuoli [2]

[1]University of Naples "Federico II", Department of Civil, Building and Environmental Engineering, Via Claudio 21, Italy

Abstract. Flow-like landslides initiated as soil slips are commonly triggered by heavy rainfall infiltrating granular and partially saturated slopes. Field monitoring of suction and water content provides valuable insights into slope responses to hydraulic loads, serving as key preparatory factors for slip initiation. However, current prediction strategies often rely on rainfall thresholds derived from empirical and statistical approaches, while integrating field monitoring into prediction procedures remains challenging. This study uses field monitoring data to develop physically based rainfall thresholds to predict shallow slips. Specifically, the short-term hydraulic response of an unsaturated slope to rainstorms was investigated in a shallow pyroclastic cover on limestone in the Lattari Mountains, Campania Region—an area highly susceptible to flow-like landslides. These field observations i) validated a numerical model predicting the slope's hydrological behaviour during rainstorms and ii) supported the development of rainfall thresholds based on mean rainfall intensity, duration, and pre-rainstorm subsoil suction. Historical landslide data from similar geological contexts were used to validate these thresholds. The study established critical surfaces in the i–d–s_0 space (mean rainfall intensity, critical duration, and antecedent suction) which can be integrated into an offline early warning procedure by combining on-site monitoring of preparatory factors with the developed thresholds.

1 Introduction

Flowlike landslides (debris flows, debris avalanches, and flowslides) often initiate as shallow slips and, due to their propagation downslope, pose significant threats to infrastructure and human lives worldwide. Such landslides are typically triggered by heavy rainfall infiltrating granular and partially saturated slopes. Field monitoring of suction and water content provides valuable insights into slope responses to hydraulic loads, serving as key preparatory factors for slip initiation [1].

Despite advancements in understanding these phenomena, the implementation of early warning systems that fully integrate in situ measurements and numerical modelling remains challenging. Current prediction strategies still predominantly rely on empirical and statistical rainfall thresholds, with limited incorporation of real-time field monitoring data [2, 3].

This study uses field monitoring data to develop physically based rainfall thresholds to predict shallow slips. Specifically, the short-term hydraulic response of an unsaturated slope to rainstorms was investigated in a shallow pyroclastic cover in the Lattari Mountains, Campania Region—an area highly susceptible to flow-like landslides. Over a two-year period, automatic field monitoring of meteorological variables, soil suction, and volumetric water content was carried out [1, 4]. These field observations i) validated a numerical model predicting the slope's hydrological behavior during rainstorms and ii) supported the development of rainfall thresholds based on mean rainfall intensity, duration, and pre-rainstorm subsoil suction. Historical landslide data from similar geological contexts were used to validate these thresholds.

This study identified critical surfaces in the i–d–s_0 space (mean rainfall intensity, critical duration, and antecedent suction), laying the foundation for an offline early warning procedure that integrates on-site monitoring of preparatory factors with physically based predictive thresholds.

2 The test site

The study area is located on the Lattari Mountains in the Campania Region (Southern Italy), specifically in the municipality of Castellammare di Stabia, Naples, as depicted in Fig. 1(a). A test site was set up on the left flank of a gully on a high elevation slope ranging from 826 to 870 m above sea level (a.s.l.). The slope angles range between 27° and 35°. The slope consists of limestones buried by a pyroclastic cover resulting from two explosive eruptions of different ages and origins. The simplified soil profile is reported in Fig. 1(c). From top to bottom, the following layers were identified: silty

* Corresponding author: marianna.pirone@unina.it

 https://doi.org/10.1051/e3sconf/202564201007

sand (designated as layers A1 and A2), white pumice from the 79 AD eruption (layer B), silty sands (pre-79 AD), and clayey silt (pre-79 AD).

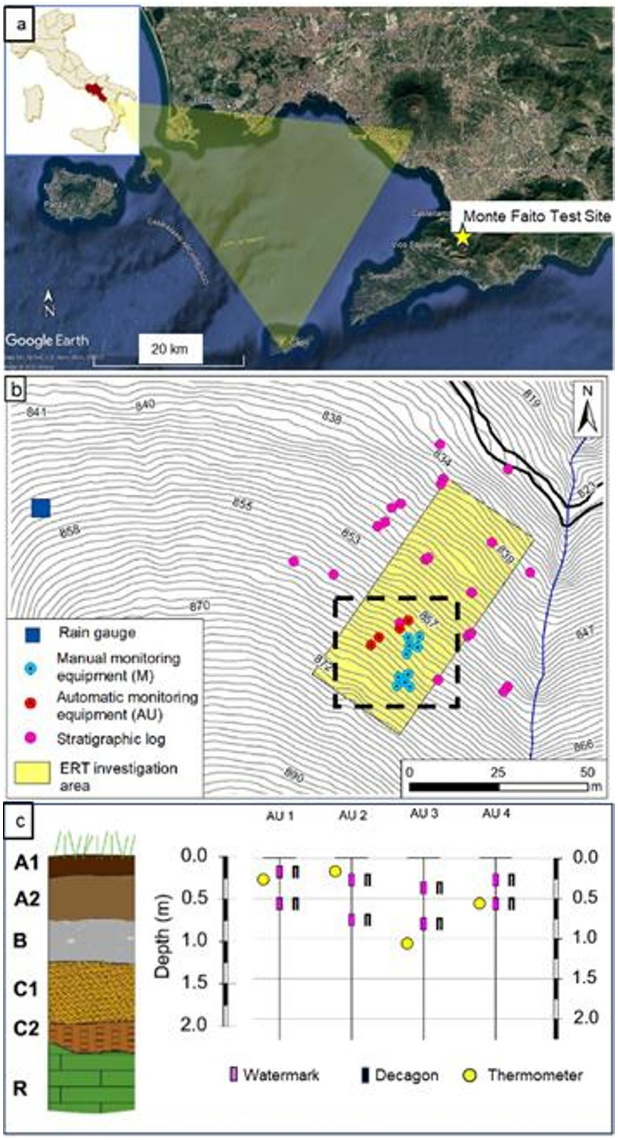

Fig. 1. (a) Location map of the Sorrento Peninsula and Lattari Mountains, highlighting the Faito test site. (b) Layout of the test site showing the positions of rain gauges, stratigraphic logs, and both manual and automatic monitoring equipment. (c) Stratigraphic profile of the Lattari Mountains indicating the installation depths of automatic monitoring instruments at the four vertical sections (AU1–AU4) (adapted from [4]).

1.1 Soil properties

Table 1 reports the mean values of the specific gravity G_s, soil porosity n, and dry unit weight γ_d, the saturated hydraulic conductivity k_{sat}, and the soil friction angle at the critical state, φ′ , as determined from laboratory-tested soil specimens. Except for layer C2, the physical and hydraulic properties are consistent with typical volcanic soils [5]. The saturated permeability values of layers A1, A2, and C1 are comparable, ranging from 5.0 × 10^{-7} to 2.0 × 10^{-6} m/s, —values in line with those measured at other test sites in the Campania Region [6-9].

The critical-state friction angle (φ′) was determined via direct shear tests on saturated samples from the upper layers (A1 and A2) and the lower layer (C1), which had average porosities of 0.68 and 0.66, respectively. Specifically, all the soils of the cover behave upon shearing as highly ductile and contractive. The measured φ′ values ranged between 35° and 39°.

Table 1. Geotechnical soil properties

Soil	Gs	n	γ_d (kN/m3)	k_{sat} (m/s)	ϕ' (°)
A1	2.60	0.65	9.10	2·10-6	38.4
A2	2.68	0.72	8.19	1.6·10-6	38.4
B	2.55	0.80	4.80	1·10-3	41.0
C1	2.65	0.66	7.35	6 10-7	35.4
C2	2.65	0.46	14.20	2.8·10-8	35.0

1.2 Field monitoring

The field instrumentation included both manual and automatic monitoring systems (Fig. 1b); this section focuses on the latter. The automatic monitoring was designed to record on an hourly basis, matric suction, volumetric water content, and soil temperature within the pyroclastic soil cover, along with meteorological variables including rainfall intensity, air temperature, relative humidity, wind speed and direction, and net radiation. A summary of the types and quantities of instruments installed at the test site, as well as the monitoring duration and data acquisition frequency, is provided in Table 2 [10].

Since seasonal fluctuations dominate the hydraulic response at depths greater than 1 m— as demonstrated by previous studies [11, 12]—only the topsoil layers (A1 and A2) were equipped with automatic sensors to capture short-term variations on an hourly scale. Four instrumented vertical profiles, labelled AU1 to AU4, were installed along the longitudinal section of the slope, as shown in Figs. 1b and 1c. The monitoring program ran from January 22, 2018, to August 1, 2019. A schematic overview of the instrumentation setup is illustrated in Fig. 1c.

Figure 2 presents the hourly time series of rainfall, matric suction, and volumetric water content recorded within the upper meter of the pyroclastic cover at one of the monitored vertical profiles (AU2) over the monitoring period from January 1, 2018, to August 1, 2019.

In Fig. 2a, rainfall is observed to occur more frequently and consistently during the autumn and winter months, with hourly intensities typically ranging between 2 and 12 mm/h. The corresponding response in volumetric water content to individual rainfall events is particularly evident at a depth of 0.20 m (Fig. 2b). For example, at this depth within the AU2 vertical profile, the volumetric water content (θ) increased from 0.39 to 0.56 following the rainfall event on February 5, 2018.

This response to rainfall becomes less pronounced with increasing depth, as seen at 0.70 m (Fig. 2c).
Seasonal fluctuations are clearly distinguishable at both depths, specifically, at 0.70 m depth their amplitudes consistently exceed those associated with individual rainfall events. This pattern is consistent with observations reported for pyroclastic covers in similar geological settings [11,12].

The hourly matric suction measurements reflect trends closely aligned with those of volumetric water content. Matric suction also exhibits seasonal oscillation, with the amplitude of variation decreasing with depth. From December through April/May, matric suction remained relatively stable, with mean values around 10 kPa.

Table 2. Description of the measurements and instruments installed at the test site.

Measure-ment	Instrument	Monitored period	Frequency
Matric suction	Granular matrix sensors n°=8	From 01-22-2018 to 08-01-2019	1 hour
Volumetric water content	Soil moisture sensors n°=8	From 01-22-2018 to 08-01-2019	1 hour
Soil temperature	Soil temperature probes n°=4	From 01-22-2018 to 08-01-2019	1 hour
Rainfall intensity	On site rain gauge n°=1	From 09-19-2017 to 07-20-2019	10 min

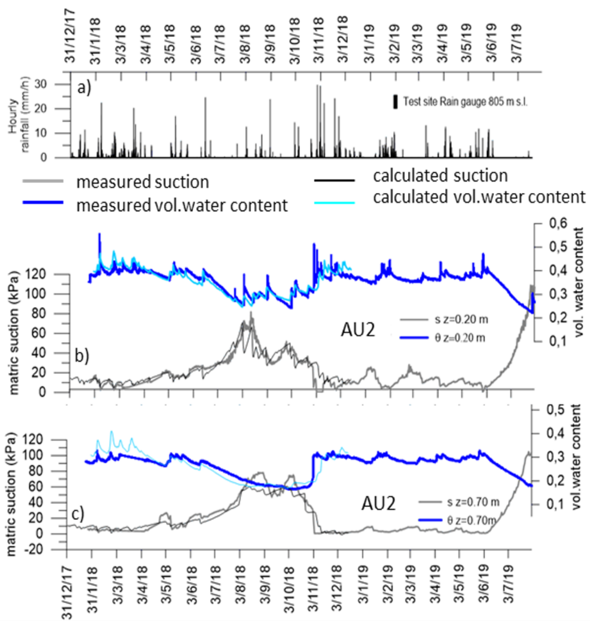

Fig. 2. Hourly rainfall (a); matric suction and volumetric water content collected at depths of (b) 0.20 m (AU2); (c) 0.70 m (AU2). The suction and volumetric water content simulated by numerical modelling are overlaid with the values measured at corresponding depths.

2 Numerical modelling

Two hydraulic numerical models, developed using the FEM code SEEP/W [13], were used to describe the infiltration phenomena in the pyroclastic slope. The first model aimed to simulate the suction–time history, capturing the long-term hydraulic behavior of the slope and assisting in calibrating its hydraulic properties. In this context, the modeled suction at vertical profile AU2 is compared to the field measurements shown in Fig. 2b and 2c, demonstrating a good match. Further details about this first model can be found in [4].

The second model, on the other hand, was designed to investigate the short-term response of the slope, particularly for predicting critical rainfall events. The results from this second model are described below.

2.1. Short-Term Slope Response under Individual Rainstorm

An equivalent infinite slope was modeled with a steepness of 34°, the mean value determined at the test site, and a thickness of 2 m (Fig. 3a). The entire soil cover was characterized by the hydraulic properties of the topsoil (A1), as the first meter of the cover is typically the layer involved in failure, according to experimental evidence [10]. The Mualem-van Genuchten model was used to define the soil water retention curve and permeability curve, with the model parameters determined by [6] and reported in Table 3.

Given that the model's purpose was to examine the effect of a single rainstorm on a pyroclastic slope as the initial suction, rainfall intensity, and rainfall duration vary, the numerical simulations focused solely on rainstorm duration, adopting hourly time-steps.

Specifically, the mean hourly rainfall intensity, i, was applied at the upper boundary, and runoff was accounted for by enabling the seepage face review option. This setting prevents the development of a water table at the soil surface. A uniform initial matric suction, s_0, was set as the initial condition before the rainstorm in all analyzed domains. It is important to note that the initial suction, s_0, within the slope reflects the slope's past hydraulic history. The lower boundary of the analysed domain was defined by the contact with a pumice layer, where suction was fixed at s_0 during all rainstorm durations that did not exceed tens of hours. By comparing the results obtained with a unit gradient and null flux at this lower boundary, it was demonstrated that assigning a constant value of s_0 at the bottom did not significantly affect the results up to half of the cover (1 m) for s_0 greater than a few kPa. At the right and left boundaries, a null flux was applied with the option for seepage face review.

First, the numerical model used to simulate the slope's response to a rainstorm was validated against several rainstorms recorded at the test site. The mean hourly rainfall intensity was applied at the upper boundary over the duration of the rainstorm, while the average field suction measured before the rainstorm at various depths was adopted as the initial condition and assigned to the lower boundary. Figure 3b validates this second numerical model by comparing field measurements with the suction values predicted by the model at the last hour of the rainstorm, at a depth of 0.70 m, for several rainstorms recorded at the test site. This comparison demonstrates that using an equivalent infinite slope with a thickness of 2 m and assuming a uniform initial suction distribution is an appropriate approach for accurately reproducing the slope's response to individual rainstorms.

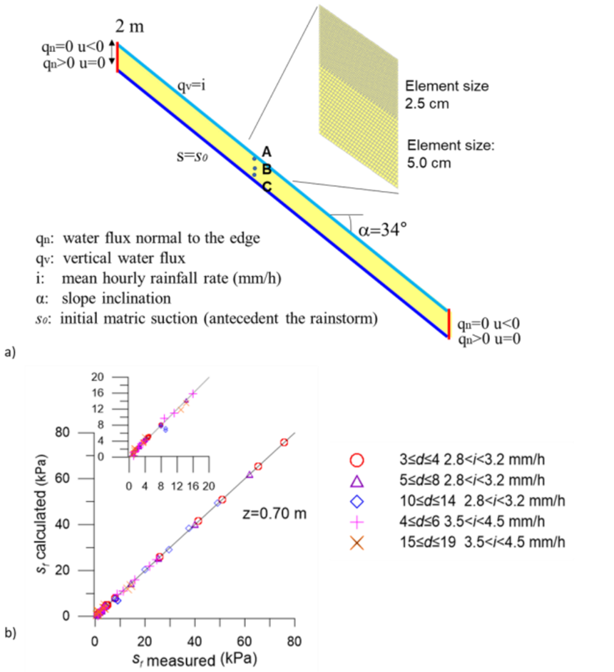

Fig. 3. (a) Geometry of the analysed slope, showing the mesh used and the assigned boundary conditions in the numerical analyses; (b) Final suction values recorded at the test site (sf measured) after various rainstorms of different durations at a depth of 0.70 m, compared with the suction values calculated by the model (sf calculated) at the same depth.

Table 3. Hydraulic parameters of the Van-Genuchten model and saturated hydraulic conductivities adopted in the numerical analyses.

Soil	θ_s	θ_r	α	n	m	K_{sat}
	-	-	1/kPa	-	-	m/s
A1	0.51	0.09	0.09	1.58	0.36	2.0E-06

2.2 Prediction of Critical Rainfall

In this section, rainstorms capable of triggering shallow slips are analyzed by considering different initial suction values (s_0) before rainstorm and slope steepness (α), ranging from 38° to 45°. To achieve this, a series of parametric analyses were performed, varying rainfall intensity, duration, initial suction, and slope steepness. A summary of all the analyses is provided in Table 4. All numerical results presented are plotted at a depth of 1 m, which is identified as the initiation depth for shallow slips in the studied geological context, based on post-landslide field observations. The results for a slope steepness of 45° are discussed here.

First, *steady-state infiltration analyses* were conducted for mean hourly rainfall intensities (i) ranging from 3 to 8 mm/h, a range selected to encompass the critical rainfall intensities recorded in the reference context. The critical value of the mean hourly rainfall intensity was assessed while disregarding the duration, assuming it to be infinite. In Fig. 4, decreases in suction (ds) calculated at a depth of 1.00 m for each rainfall intensity (i) are plotted against the initial suction (s_0), which influences the steady-state solution as it is imposed at the lower boundary. In Fig. 4, the red line, denoted $ds_c - s_{0c}$ and referred to as the critical line, represents the envelope for which FS =1, where FS is the safety factor of an infinite slope. The soil shear strength under partially saturated conditions was calculated using Bishop's principle of effective stresses; then, the critical line was determined by calculating the critical value of suction, denoted s_c, causing FS = 1; hence, the FS at a depth of 1 m was as follows:

$$FS=(\gamma\cdot 1\cdot \cos^2\alpha+S_c\cdot s_c)\cdot \tan\varphi'/(\gamma\cdot 1\cdot \cos\alpha\cdot \mathrm{sen}\alpha) \quad (1)$$

$$ds_c=s_{0c}-s_c \quad (2)$$

$$S_c=\theta_c/n \quad (3)$$

where S_c = the degree of saturation determined from the volumetric water content, θ_c, corresponding to s_c adopting the mean soil porosity of layer A1, n, which is 0.65. The value of θ_c was determined from the modeled retention curve in Table 3 corresponding to s_c.

In Fig. 4, s_c is represented by the intersection of the red curve with the horizontal axis. Subsequently, Eq. (2) establishes the critical value of suction decrease, ds_c, as s_0 varies, assessing a linear relationship between these variables. The intersection between the curves associated with different mean hourly rainfall intensities i and the critical line provides the maximum s_0 value for which the considered rainfall intensity could trigger shallow slip and is denoted $s_{0c\_steady\_i}$. In other words, for $s_0 > s_{0c\_steady\_i}$, a rainstorm of intensity i is not critical regardless of its duration. Based on the steady-state infiltration analyses, it is evident that a mean hourly rainfall intensity of 3 mm/h is never critical for the slopes in question. In contrast, rainstorms with i≥ 4 and i ≥ 5 mm/h are critical when the steady-state initial suction (s_{0c_steady}) is less than 5.5 kPa and 13 kPa respectively. It is also noteworthy that the curves for rainfall intensities of 6 and 8 mm/h overlap because both exceed the saturated permeability limit; under steady-state conditions, any excess rainfall beyond the slope's absorption capacity runs off the slope. Thus, studying the hydromechanical behavior of slopes under steady-state conditions allows us to eliminate hourly rainfall intensities, as a function of s_0, that would not trigger a shallow slip, even for theoretically infinite durations.

The *transient analyses* were carried out for rainfall intensities ranging from 4 to 8 mm/h, which are considered critical for the slope. In Figure 5, for intensity

(i) equal to 4 and 5 mm/h, the suction decreases (ds) are plotted against the initial suction (s_0) for durations of 3, 6, 12, 18, and 24 hours, assuming a slope steepness of α = 45°. As in the steady-state analysis, the critical line is overlaid on the ds–s_0 curves determined through the transient analyses.

Table 4. Summary of numerical analyses performed, including assigned boundary and initial conditions, as well as the adopted slope inclinations.

Rainstorm	Type of analysis	Initial matric suction, s_0 (kPa) (uniform distribution)	Slope Inclination (°)
i=4 mm/h *d*:24 h	Steady state/ Transient state	2-3.6-5-10-15-20-25-30-40-50-60-75-100	34,38, 40,42,45
i=5 mm/h *d*:24 h	Steady state/ Transient state	2-3.6-5-10-15-20-25-30-40-50-60-75-100	34,38, 40,42,45
i=6 mm/h *d*:24 h	Steady state/ Transient state	2-3.6-5-10-15-20-25-30-40-50-60-75-100	34,38, 40,42,45
i=8 mm/h *d*:24 h	Steady state/ Transient state	2-3.6-5-10-15-20-25-30-40-50-60-75-100	34,38, 40,42,45
i=3 mm/h	Steady state	2-3.6-5-10-15-20-25-30-40-50-60-75-100	34,38, 40,42,45

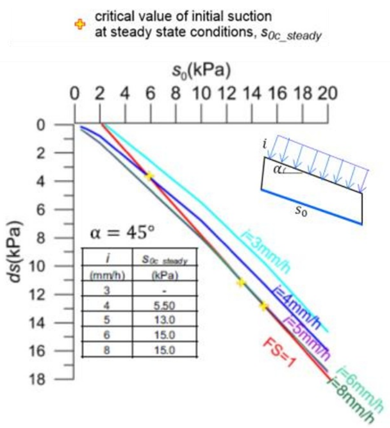

Fig. 4. Results of numerical analyses under steady-state conditions. The red line (FS = 1) represents the critical combinations of suction decrease (d_{sc}) and initial suction (s_{0c}) that correspond to a factor of safety equal to one for the infinite slope model. The accompanying tables report the critical initial suction values (s_{0c_steady}) associated with each analyzed mean hourly rainfall intensity.

The intersection of the critical line with the curves obtained under transient conditions defines the critical duration of each rainfall event as a function of the initial suction within the slope. As illustrated in Fig. 5, for instance, a rainfall intensity of 4 mm/h becomes critical only for initial suction values (s_0) lower than approximately 2.5 kPa and for relatively short durations. For an intensity of 5 mm/h, the critical condition is met when $s_0 < 3$ kPa; however, a modest increase in initial suction—from 3.00 to 6.00 kPa—results in a significant extension of the critical duration, from 3 to 18 hours [see Fig. 5(b)].

Figure 6 summarizes the results of the transient analyses. Specifically, it shows the pairs of critical initial suction s_{0c} and critical rainfall duration d_c for each rainfall intensity, ranging from 4 mm/h to 8 mm/h. The minimum value of s_{0c} corresponding to null rainfall (d_c =0) and unit safety factor for infinite slope with α=45°, is 2.1 kPa. The area above each curve represents stable conditions. As expected, for low initial suction values between 2 and 3 kPa, only a few hours of rainfall (3 to 4 hours) are sufficient to trigger instability. Moreover, these critical initial suction values of few kPa show little sensitivity to rainfall intensity.

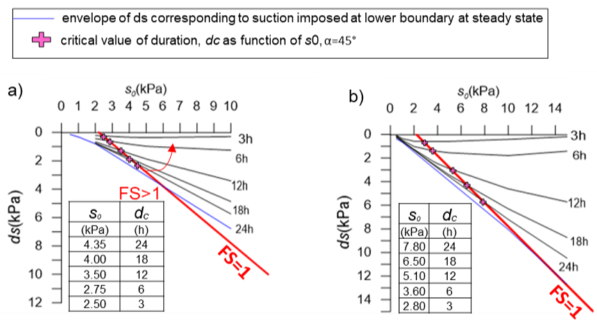

Fig. 5. Results of numerical analyses under transient conditions: decrease in suction (ds) plotted against initial suction (s_0) for a slope inclination α = 45°, and rainfall intensities of (a) 4 mm/h; (b) 5 mm/h. The critical line corresponding to FS = 1 is superimposed on each chart.

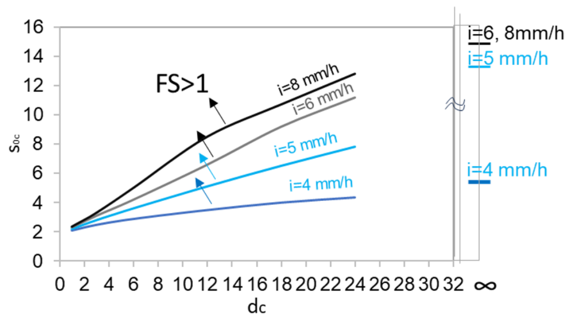

Fig. 6. Results of numerical analyses under transient conditions for a slope inclination α = 45°: critical initial suction s_{0c} against critical rainfall duration for rainfall intensities from 4 to 8 mm/h.

3 Multi-Factor Rainfall Thresholds

The sets of mean hourly intensity (i), critical duration (d_c), and initial suction corresponding to d_c, determined by intersecting the critical line with the ds–s_0 curves

resulting from transient analyses (Fig. 5, 6), were used to develop critical surfaces in the 3D i–d–s_0 space.
Fig. 7a shows the surface obtained for slope inclinations of 45°. It can be regarded as multifactor thresholds, delineating the space encompassing the critical intensity durations for nonhazardous events. Again, looking at Fig. 7a, it is possible to detect for infinite duration d the maximum critical value of s_0, named as $s_{oc\ steady}$ and the minimum critical value of i_c, that allow or prevent slip initiation. In Figs. 7a, these values are represented as vertical and horizontal plane, respectively (colored transparent surfaces).

In Fig. 7b, the i_c–d curves for different values of s_0 obtained from the intersection of the critical surface for α =45° with vertical planes at constant values of s_0 equal to 5 and 10 kPa, are plotted. The i_c–d curves exhibit a strongly nonlinear trend in the range of short durations and tend toward a constant value of i, indicating the minimum value capable of triggering shallow slip. The recorded rainfall events that did not trigger failure during the monitoring period, corresponding to measured initial suctions of 5 and 10 kPa are plotted in Fig. 7b. They are always positioned below the corresponding thresholds, indicating they were not critical, as confirmed by experimental evidence. Then, critical events triggering flowlike landslides at the Lattari Mountains for which 5 ≤ s_0 ≤ 10, as determined by numerical back-analyses [7] are also superimposed. The critical events that occurred for s_0=5 kPa are surprisingly very close to the thresholds determined for 5 kPa; the same occurs for s_0 =10 kPa.

Therefore, curves i_c–d include critical events, proving the good performance of the model and indicating that each critical event likely starts from a different s_0 [14].

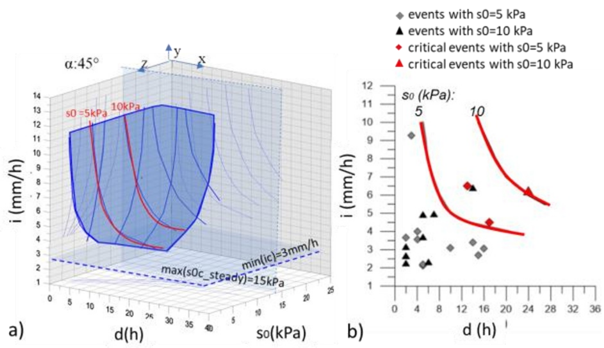

Fig. 7. a) Multifactor critical surfaces determined by the triplets i_c–d_c–s_0 that are able to trigger shallow slip in the infinite slope with α = 45°; b) intersection of the critical surface in a) with vertical planes at constant values of s_0, 5 and 10 kPa, along with recorded rainfalls corresponding to similar s_0 values and historical critical events.

4 Discussion and Conclusion

The on-site measurement data set was used to calibrate a numerical infiltration model designed to predict critical rainfall by varying the suction before the event and the slope steepness.

Despite being a simple model applied to an infinite slope; it incorporates the key factors influencing shallow slip initiation. Through a progressively challenging approach, it was first possible to define, for each mean rainfall intensity, the maximum initial suction, $s_{0c\ steady\ i}$, critical for initiation under infinite duration through a steady-state analysis. Then, the critical duration, d_c, for each pair of s_0 and mean intensity, i, was determined through transient analysis. By using this approach, multifactor rainfall thresholds were developed in the i–d–s_0 space. This work emphasizes that physically based rainfall thresholds adequately consider the role of the soil slope; thus, it is impossible to disregard the initial hydraulic conditions within the slope.

References

[1]. M. Pirone, R. Di Maio, G. Forte, C. De Paola, E. Di Marino, R. Salone, A. Santo, and G. Urciuoli. 2023. Eng. Geol. **315** (Mar): 107045 (2023)

[2]. L. Piciullo, S. L. Gariano, M. Melillo, M. T. Brunetti, S. Peruccacci, F. Guzzetti, and M. Calvello. Landslides **14** (3): 995–1008 (2017)

[3]. F. Guzzetti, S. Peruccacci, M. Rossi, and C. P. Stark. 2007. Meteorol. Atmos. Phys**. 98** (Dec): 239–267 (2007)

[4]. M. Pirone, G. Forte, A. Santo, and G. Urciuoli. J. Geotech. Geoenviron. Eng. **151** (3) (2025)

[5]. M. Pirone, R.Papa, M.V. Nicotera. Unsaturated Soils - Proceedings of the 5th International Conference on Unsaturated Soils, 2, pp. 1273-1278. ISBN: 978-041560430-7 (2011)

[6]. A.S. Dias, M. Pirone, M. V. Nicotera, and G. Urciuoli. Geomech. Energy Environ. **30** (Jun): 100235 (2022)

[7]. A.S. Dias, M. Pirone, M. V. Nicotera, and G. Urciuoli. Acta Geotech. 17 (3): 837–855 (2022)

[8]. M.V. Nicotera, R. Papa, and G. Urciuoli. Eng. Geol. **195** (Sep): 70–84 (2015)

[9]. E. Damiano, L. Olivares, and L. Picarelli. Eng. Geol. **137** (Jun): 1–12 (2012)

[10]. S. Guglielmi, M. Pirone, A. S. Dias, F. Cotecchia, and G. Urciuoli. J. Geotech. Geoenviron. Eng. **149** (11):05023005 (2023)

[11]. L. Comegna, E. Damiano, R. Greco, A. Guida, L. Olivares, and L. Picarelli. 2016. Can. Geotech. J. **53** (7): 1125–1137 (2016)

[12]. M. Pirone, R. Papa, M. V. Nicotera, and G. Urciuoli. Landslides **12** (2): 259–276 (2015)

[13]. J. Krahn. Seepage modeling with SEEP/W: An engineering methodology. Calgary, AB, Canada: GEO-SLOPE International (2004)

[14]. Pirone, M. Ph.D. thesis, Dept. Of Civil, Building and Environmental Engineering, Università degli Studi di Napoli Federico II. (2010)